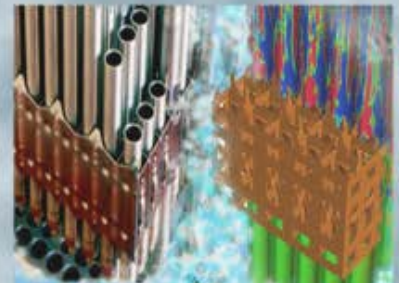
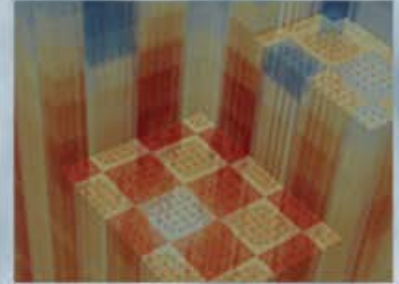


COBRA-TF Parallelization and Application to PWR Reactor Core

Vefa Kucukboyaci and Yixing Sung
Westinghouse Electric Company

Robert Salko
Oak Ridge National Laboratory

April 19, 2015



COBRA-TF PARALLELIZATION AND APPLICATION TO PWR REACTOR CORE SUBCHANNEL DNB ANALYSIS

Vefa Kucukboyaci and Yixing Sung

Westinghouse Electric Company
1000 Westinghouse Drive, Cranberry Woods, PA, 16066 USA
kucukbvn@westinghouse.com; sungy@westinghouse.com

Robert Salko

Oak Ridge National Laboratory
Oak Ridge, TN, 37831, USA
salkork@ornl.gov

ABSTRACT

COBRA-TF (Coolant Boiling in Rod Arrays – Two Fluid) or CTF is a transient subchannel code, selected to be the reactor core thermal hydraulic (T/H) simulation tool in the multi-physics code, Virtual Environment for Reactor Applications Core Simulator (VERA-CS) development project of the Consortium for Advanced Simulation of Light water reactor (CASL) sponsored by the US Department of Energy. CTF has been improved and parallelized by CASL as part of its multi-physics software package to help the nuclear industry address operational and safety challenge problems, such as departure from nucleate boiling (DNB). In this paper, CTF's performance and capability are evaluated by modeling and analyzing full core 3D models of a 3-loop and a 4-loop pressurized water reactor (PWR) with all fuel assemblies modeled in subchannels. Calculations have been performed for DNB ratio (DNBR) predictions in complete loss-of-flow, low-flow main steam line break, and rod ejection at full power transients. Those applications demonstrate CTF's capabilities for modeling the entire reactor core in subchannels and simulating challenging PWR transients in preparation for coupled multi-physics analysis using the VERA-CS neutronic and T/H code system.

Key Words: DNB, COBRA-TF, Subchannel, Parallel

1 INTRODUCTION

An advanced integrated modeling/simulation tool suite is currently under development through the Consortium of Advanced Simulation of Light water reactors (CASL), aiming to increase the competitiveness of the US nuclear power generation by solving operational and safety challenge problems, while enhancing safety, and reducing cost. The 3D subchannel thermal hydraulic code, COBRA-TF (CTF) [1, 2], is part of the integrated simulation tool, named Virtual Environment for Reactor Applications (VERA) [3] in the CASL program. CTF is coupled with reactor neutronics codes in the VERA-CS package to simulate reactor coolant flow and to determine the key limiting phenomena in nuclear power plant operations and safety.

DNB is one of the challenge problems that CASL is addressing in support of designs and analyses of the PWR fuel, reactor reloads, non-LOCA accidents, plant operation, and protection systems. DNB, also known as local clad surface dryout, affected by detailed flow patterns and mixing, causes dramatic reduction in heat transfer during transients (e.g., overpower and loss of coolant flow) leading to high cladding temperatures. Most PWR fuel assemblies contain features

to enhance DNB performance (e.g., mixing vane (MV) grid spacers). Reactor reloads are designed to meet design limits (e.g., fuel rod power peaking factor limit, $F_N\Delta H$) to ensure adequate margins to DNB are retained. Accident analyses are performed to confirm that the DNB acceptance criterion is met during non-LOCA events (e.g., steam line break transients). DNB-related limits are specified and monitored per operating procedures and specifications (e.g., core thermal limits defined as coolant operating temperature versus power level at different pressure). Reactor trip and protection systems are designed to prevent DNB occurrence during operations and accident conditions (e.g., the Over-Temperature Delta-T (OTΔT) trip for Westinghouse designed PWRs).

CASL's mission is to develop the methods and tools to help the nuclear industry address the DNB challenge problem. Simulation capability targets aimed by CASL include creation of validated tools coupled to detailed pin-resolved radiation transport and fuel performance models to predict DNB using methods that are more advanced to evaluate safety margin, enhance understanding, and evaluate impact of spacer grid design features. In this paper, CTF's capability for transient fuel rod and subchannel analyses, including DNBR prediction, is evaluated as a stand-alone code by modeling and simulating full core 3D models of a 3-loop and a 4-loop PWR with each fuel assembly modeled in subchannels. Simulations are performed for DNB accidents such as complete loss-of-flow, low-flow main steam line break, and rod ejection at full power transients. Those applications demonstrate CTF's capabilities for modeling the entire reactor core in subchannels and simulating challenging PWR transients accurately and efficiently.

2 COBRA-TF PARALLELIZATION

2.1 CTF Overview

CTF is the shortened name given to the version of COBRA-TF being jointly developed by Pennsylvania State University (PSU) and Oak Ridge National Laboratory (ORNL) [1, 2] under sponsorship of the Department of Energy (DOE) CASL Energy Innovation Hub. CTF is a thermal-hydraulic simulation code designed for light water reactor (LWR) vessel analysis. It uses a two-fluid, three-field modeling approach to model the independent behavior of liquid, droplets, and vapor.

Pacific Northwest National Laboratory developed the original COBRA-TF code as a thermal-hydraulic rod-bundle analysis code in 1980 under the sponsorship of the Nuclear Regulatory Commission (NRC) [4]. It was subsequently implemented in the COBRA-TRAC code system [5] and further validated and refined as part of the FLECHT-SEASET 163-Rod Blocked Bundle Test and analysis program [6]. After making numerous improvements, PSU re-branded their version of the code as CTF. In 2012, the code was adopted into the CASL program, where it is currently serving as the subchannel thermal-hydraulics component of VERA-CS.

Since its inclusion into the CASL program, the code has undergone a number of additional improvements, some of which include:

- Development of a PWR preprocessor utility [14] for user-friendly, rapid generation of CTF models of PWR designs,
- Inclusion of native visualization capabilities,

- A number of source-code optimizations for the reduction of code memory usage and execution time,
- Full distributed-memory parallelization of the code,
- Application of source code controls using the Git version control system,
- Integration into an automated build and testing system using CMake and Tribits [8],
- Coupling to other packages for solving reactor kinetic behavior and fuel performance [7],
- Performance of a code validation study [9].

In addition to the numerous code feature improvements, an automated regression and unit testing test suite has been developed for the code that is run on a continuous basis on servers at ORNL to protect code features and ensure continuous proper functioning of the code.

2.2 CTF Parallelization

CTF and other subchannel codes allow the user to lump rod-bundle coolant channels and fuel rods into a reduced set of entities in the computational model. Using this feature, coarse-mesh models can be generated where a flow channel in the code model, for example, may represent an entire fuel assembly in the reactor being modeled. While allowing for very fast-running simulations, this approach has the adverse effect of reducing accuracy by smearing the finer details in the simulation. A goal of CASL is to create high-fidelity modeling and simulation capabilities; so it was desirable to create coupled neutronic and T/H reactor models on a pin-cell basis, meaning that each coolant channel in the rod bundle is represented by a subchannel in CTF.

This posed two primary challenges: (1) creating a CTF input deck was a labor intensive and error prone process, even for moderately sized models (e.g. single 17x17 assembly), and (2) the resulting high-resolution, full core model may contain millions of mesh cells, which was a computationally expensive problem to solve. The first challenge was met through development of a separate preprocessor utility that takes a simplified input deck containing general geometric information (e.g. rod pitch, bundle pitch, core and assembly maps), and produces a CTF input deck for the model. The second challenge was met through two stages. First, a set of code optimizations was made to reduce serial code memory usage and execution time [10]. While results of this effort were impressive, leading to 9x reductions in execution time, large-scale, quarter-symmetry models (~500,000 mesh cells) were still taking roughly 4 hours to reach convergence on the ORNL development cluster. Therefore, a second step was taken to improve runtime by parallelizing the code [11].

A domain decomposition approach targeting distributed memory machines was chosen for doing the parallelization. This approach was performed with intention of scaling up to machines with hundreds of cores. The actual domain decomposition is performed by the preprocessor utility, which performs the decomposition on a per-assembly basis. In other words, each fuel assembly in the core becomes a solution domain, solved by an individual processor in the simulation. An example decomposition of a 5-assembly model of 3x3 assemblies is shown in Figure 1, with each of the five colors representing a different solution domain. This decomposition strategy was chosen due to its ease of implementation; however, it does have a drawback in that the number of cores used for the simulation must match the number of

assemblies in the model. For example, a 193-assembly, full core model must be run with 193 cores.

By using a domain decomposition approach, nearly the entire code execution is done in parallel, with one notable exception being writing of code output. Since assemblies/domains can communicate with one another in the lateral direction, it is necessary to share data between the domains. This was achieved by creating “ghost” channels and rods around the bounding edge of each domain. No solution is performed in the ghost entities of a given domain; rather, they are simply containers for boundary data. The ghost entities have their data periodically updated throughout the CTF solution algorithm using the message passing interface (MPI). Data is passed from the domain that owns the given entity to the domains that are “ghosting” that entity.

A pivotal point in the CTF solution algorithm is the solution of a system pressure matrix, which ties the momentum equations to the mass/energy equations by correcting the pressure and, thus the velocity, in order to preserve continuity. This set of equations must be solved simultaneously. This task was achieved with the use of the Portable, Extensible Toolkit for Scientific Computation (PETSc) [12]. The pressure matrix is built and solved in parallel in PETSc using a bi-conjugate gradient stabilized (BiCGStab) solver.

To complete this work, verification and scaling studies were performed. The verification studies involved checking that parallel and serial simulation results were identical for a collection of CTF models; this ensures that the integrity of the CTF solution algorithm has been maintained during the parallelization work. The scaling study involved timing sections of the code for problems of increasing size on one of the Oak Ridge Leadership Computer Facility (OLCF) clusters. Figure 2 shows the increase in wall time in selected sections of the code execution for problems of increasing size. The model size increased from 1 to 193 17x17 assemblies. Because the file output step is done in serial, its computational time increased linearly with model size. During a coupled simulation, where CTF will be executed multiple times during the simulation, this file output cost is paid only once at the end of the simulation.

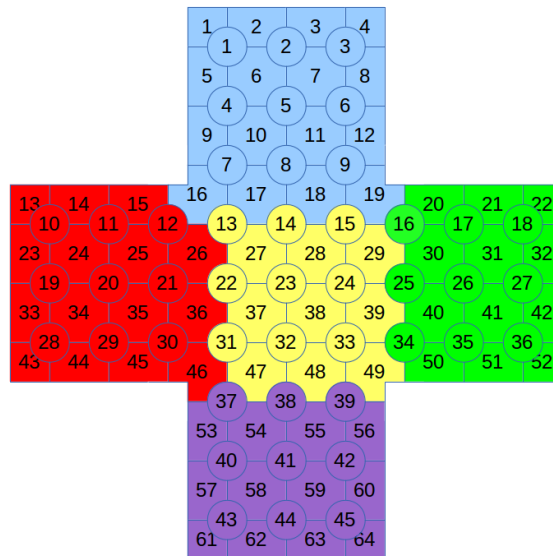


Figure 1. Example domain decomposition for 5 3x3 assemblies

Most importantly, this figure demonstrates that a quarter-core, pin-resolved model with 500,000 mesh cells that took 4 hours to solve in serial, can now be solved in about 10 minutes in parallel. This significant improvement in runtime resulted in CTF becoming a practical tool for large-scale, high-resolution models.

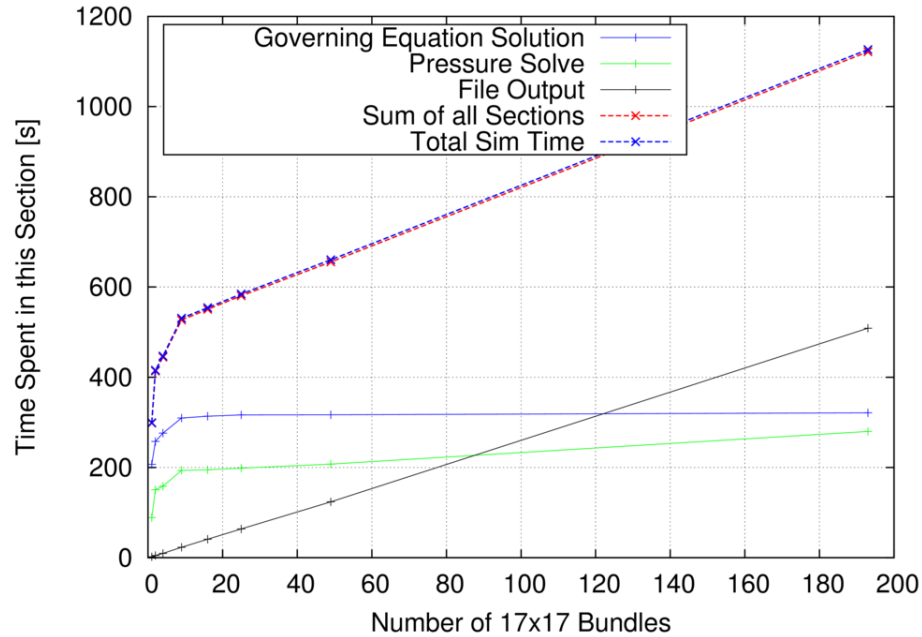


Figure 2. Weak scaling study of parallel CTF on OLCF Titan Cluster

3 DEMONSTRATION OF DNB ANALYSIS IN A REACTOR CORE

In parallel to the software improvements, CTF code functionalities and capabilities were evaluated and assessed for CASL challenge problem applications. After the transient predictive capabilities of CTF were assessed for simple benchmark problems, such as the TK tests (single channel/single rod) [13], the size and the complexity of the CTF model were then increased to simulate an actual PWR core in transient calculations, in order to evaluate the adequacy of the models and to assess the capabilities and the performance of CTF with a large model. For this purpose, three typical PWR DNB-related transient cases were analyzed using a full 3D core T/H model in subchannels: Complete loss of flow (LOF) transient, main steam line break (MSLB), and rod ejection reactivity insertion accident (RIA) transient initiated at power.

3.1 Reactor Core and Fuel Description

A 4-loop core for the LOF and RIA transients and a 3-loop core for the MSLB analysis were chosen for this study. Each core type used a Westinghouse 17x17 fuel assembly design with a fuel rod outside diameter of 0.374 inches (9.5mm). In this fuel design, there are 264 fuel rods, 24 guide tubes, and 1 instrument tube, as seen in Figure 3. Eleven spacer grids including 6 mixing-vane (MV) grid spacers and 3 intermediate flow mixer (IFM) grid spacers are located at certain elevations and inlet and outlet nozzles are at the bottom and top of the fuel assembly.

Table I shows the design data for the Westinghouse 17x17 robust fuel assembly (RFA) fuel assembly. The 4-loop core and the 3-loop core have 193 and 157 of these fuel assemblies, respectively. Table II shows the initial operating and boundary conditions for the 4-loop core for the LOF and RIA transients. Initial and boundary conditions for the MSLB transient are discussed in Section 3.4.

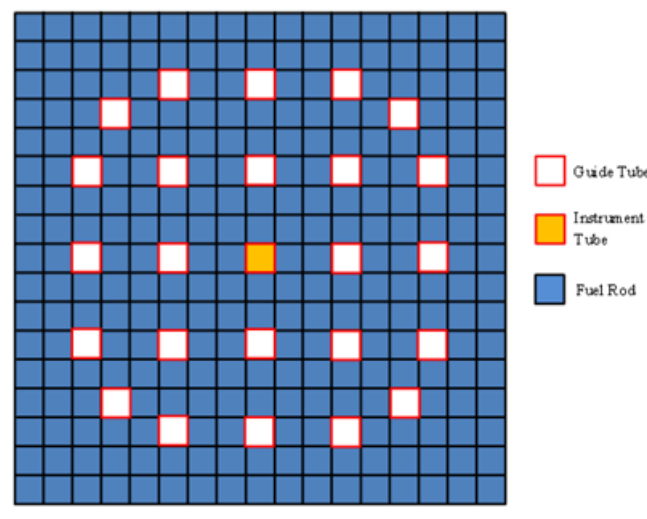


Figure 3. 17x17 Fuel Assembly Fuel Rod, Guide and Instrument Tube Pattern

Table I: Westinghouse 17x17 Assembly Design Description

Parameter	Unit	Value
Active Core Length	in	144
Rod Pitch	in	0.496
Clad Material		Zirc
Clad Outer Diameter	in	0.374
Clad Thickness	in	0.0225
Fuel Material		UO ₂
Pellet Outer Diameter	in	0.3225
Guide Thimble Material		Zirc
Guide Thimble Thickness	in	0.020
Guide Thimble Outer Diameter	in	0.482
Instrument Tube (IT) Material		Zirc
IT Thickness	in	0.020
IT Inner Diameter	in	0.442
Assembly Pitch	in	8.466

Table II: Initial and Boundary Conditions

Parameter	Unit	Value
Inlet Temperature	°F	544
System Pressure	psia	2250
Inlet Flow Rate	lb/s	178.054
Assembly Power	MW _{th}	22.465

3.2 Model Approach

Using the CTF preprocessor [14] and the data from Table I and Table II, a full core model was created for the 4-loop plant. Figure 4 shows the 4-loop core model, from the single subchannel in a fuel assembly to the entirety of the core. The 4-loop core model had 56,288 channels, 112,064 gaps, 50,952 fuel rods, and 4,825 guide/instrumentation tubes. Each fuel rod was modeled using 6 radial nodes in the pellet and 2 in the clad, and 151 axial nodes, leading to total of 8.5 million mesh cells in the 4-loop model. The average linear heat rate was set to 5.83kW/ft. A constant pellet-to-clad gap conductance was used in the fuel rods. The transient simulations used a variable time step size, from a minimum of 1E-6 second to a maximum of 1E-1 second.

The 3-loop core model, used for the low-flow steamline break case, had 45,884 channels, 91,256 gaps, 41,448 fuel rods, and 3,925 guide/instrumentation tubes, leading to 6.9 million mesh cells. For steady-state convergence (used in the MSLB case), global energy and mass balance criteria were set to 0.01%, while fluid and solid energy and mass storage criteria were set to 0.5%.

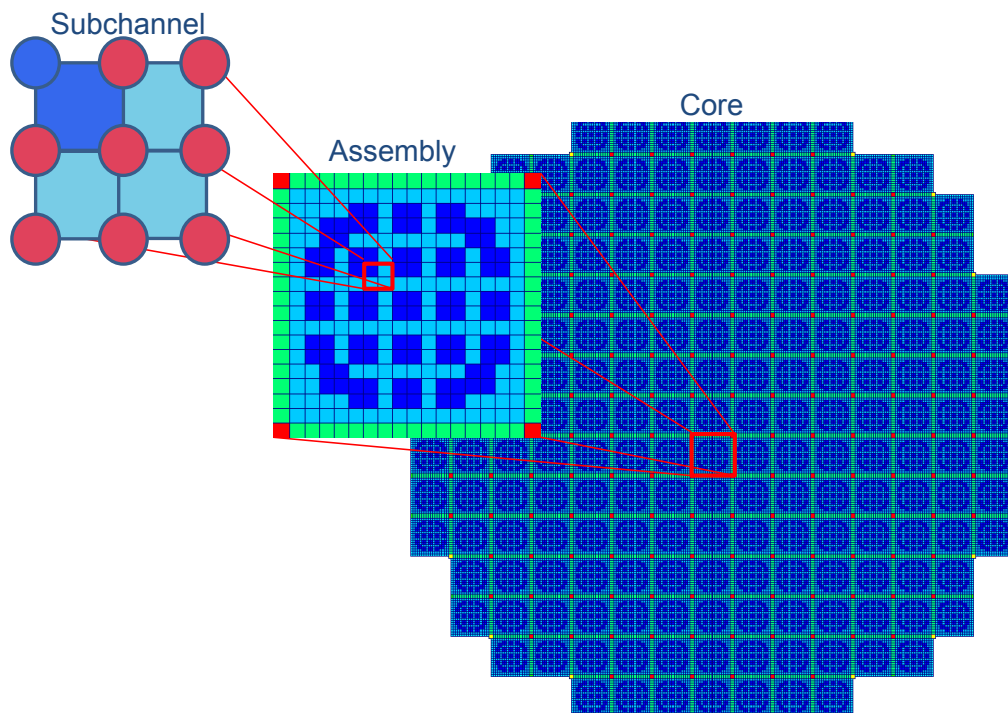


Figure 4. 3D Full Core Model for the 4-Loop Plant Pattern

3.3 DNBR Prediction for Complete Loss of Flow Transient

A complete loss of forced reactor coolant flow may result from a simultaneous loss of electrical supplies to all reactor coolant pumps (RCPs). If the reactor is at power at the time of the accident, the immediate effect of loss of forced reactor coolant flow is a rapid increase in the reactor coolant temperature and subsequent increase in reactor coolant pressure. The flow reduction and increase in coolant temperature may eventually result in DNB. The objective of this study is to demonstrate that DNB criterion is met in this complete loss of flow transient.

Figure 5 shows the core radial power distribution determined from stand-alone 3D nodal diffusion calculations, simulating core depletion and power history. Because all 4 pumps are assumed to have lost power, the problem is symmetric. Nevertheless, this full core model is well suited to assess the capability of CTF for solving large scale problems. As the figure indicates, in this low leakage pattern, the higher power assemblies were located in the middle 1/3rd ring of the core and the hot assembly power factor was about 1.28. Figure 6 shows the pin power distribution within the fuel assembly. Intra-assembly power distribution is also obtained from the 3D nodal calculations by pin-power reconstruction methods using assembly data generated by a lattice physics code. The fuel rod power peaking factor within the hot assembly was about 1.06. A modified chopped cosine axial power shape with a slight top peak, as seen in Figure 7, was applied to the whole core.

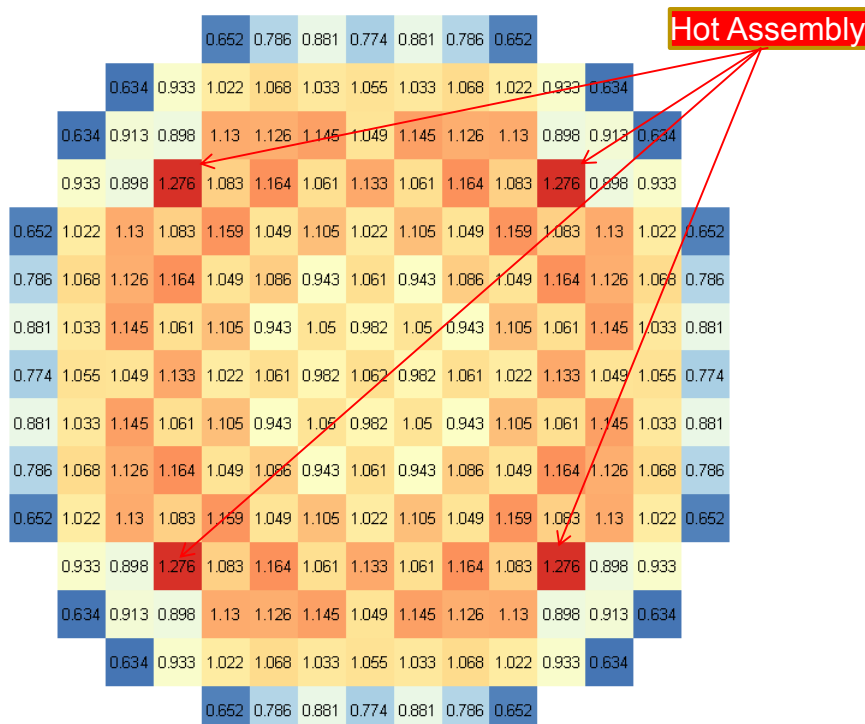


Figure 5. Core Radial Power Distribution Used in the 4-Loop Plant Model

Flow and power forcing functions as determined from a transient analysis using a systems code were applied to calculate the DNBR values at each time step. The W-3 DNB correlation, which did not take credit of the mixing vane benefit, was conservatively used for the DNBR calculation. Note that the system pressure and the inlet temperatures were assumed to remain

constant at their initial values. Figure 8 shows that while the core inlet flow rate decreased substantially within the first few seconds; there was a time delay until the core trip occurred. Because of the flow-to-power mismatch during this period, the DNBR decreased to a minimum value of about 1.6. Once the core power was reduced after the reactor trip, the DNBR margin increased again and the transient was terminated. The maximum clad temperature remained virtually unchanged, only shifting in the axial location, as shown in Figure 9. Channel liquid velocities and mixture temperatures at different times into the transient are shown in Figure 10 and Figure 11, respectively. Consistent with the inlet flow, the liquid velocity decreases gradually; the decrease in flow propagates from the bottom of the core to the top. The initial uniform distribution is replaced by a distribution that is proportional to the power distribution. Conversely, the mixture temperatures, as shown in Figure 11, start increasing with the decreasing flow. Except for the low power peripheral channels, the 3D plot indicates that most of the channels quickly reach saturation temperatures at about 3ft from the bottom and remain at saturated conditions.

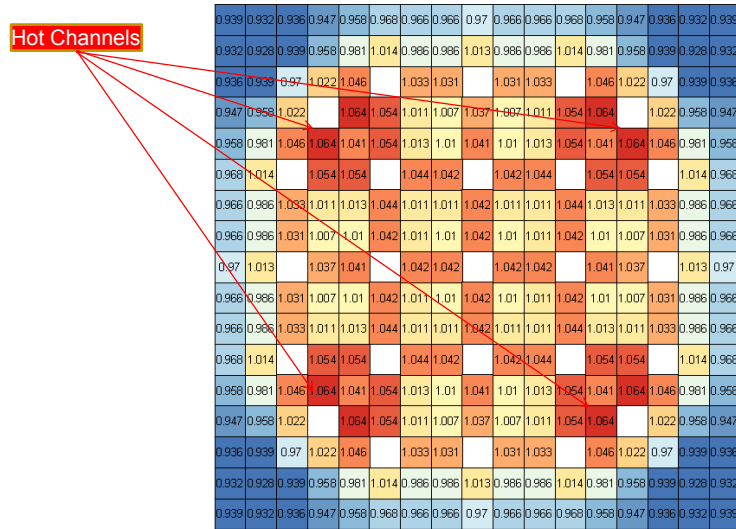


Figure 6. Assembly Power Distribution Used in the 3D simulations

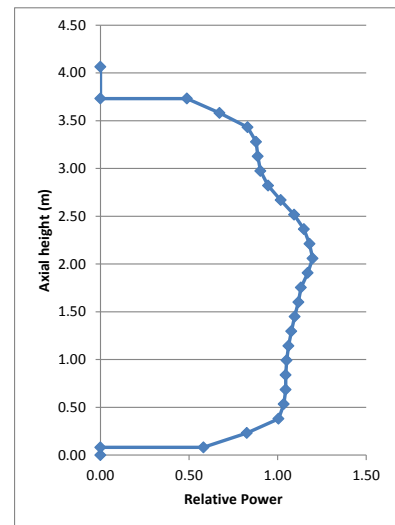


Figure 7. Axial Power Profile Used in the 4-Loop Core Model

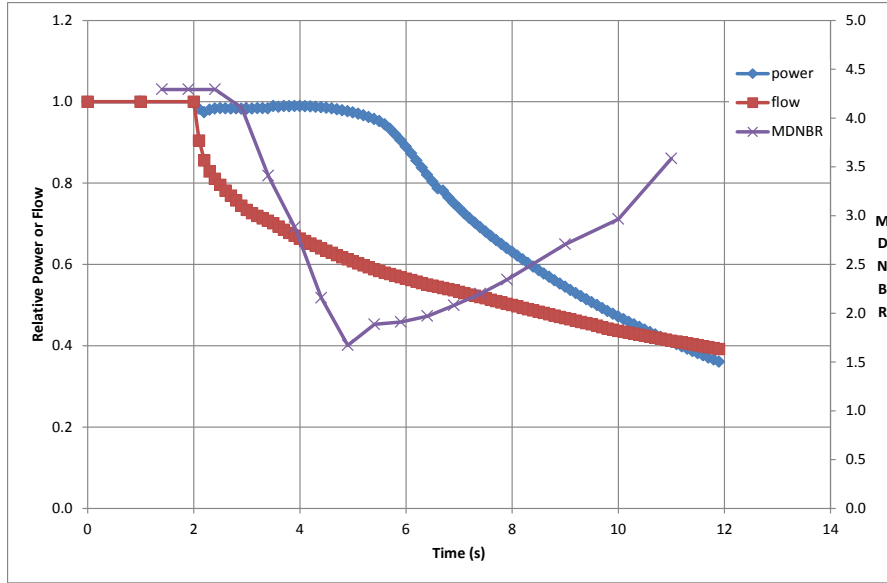


Figure 8. Flow, Power, and MDNBR as a Function of Time in the LOF transient

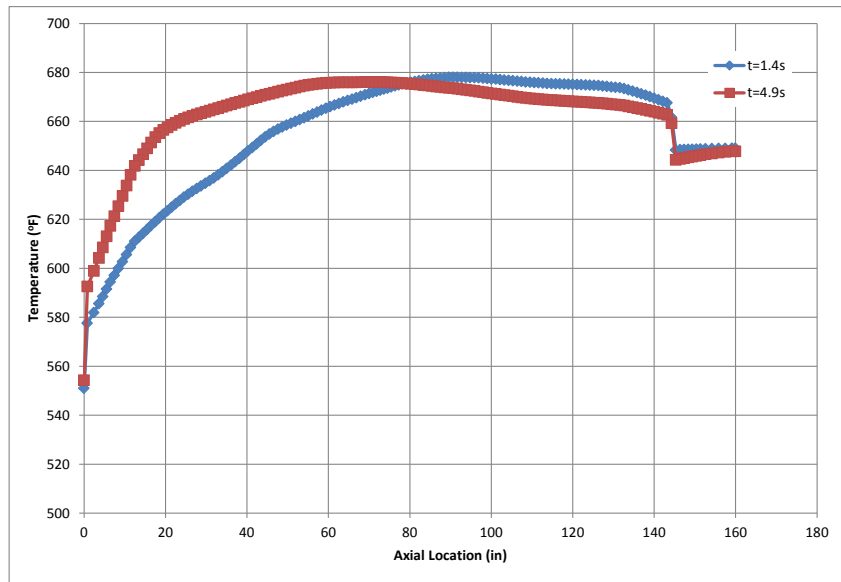


Figure 9. Hot Channel Clad Surface Temperatures at T=1.4 s (initial) and T=4.9 s (at MDNBR)

This transient was simulated on 193 compute nodes (1 fuel assembly/node), accessing the memory of 2 cores/node to accommodate the large problem size. The total wall-clock time for this 12second transient was ~ 8hours. The analysis performed has demonstrated that CTF is capable of performing DNBR calculations in the entire core for a complete loss of forced reactor coolant flow transient.

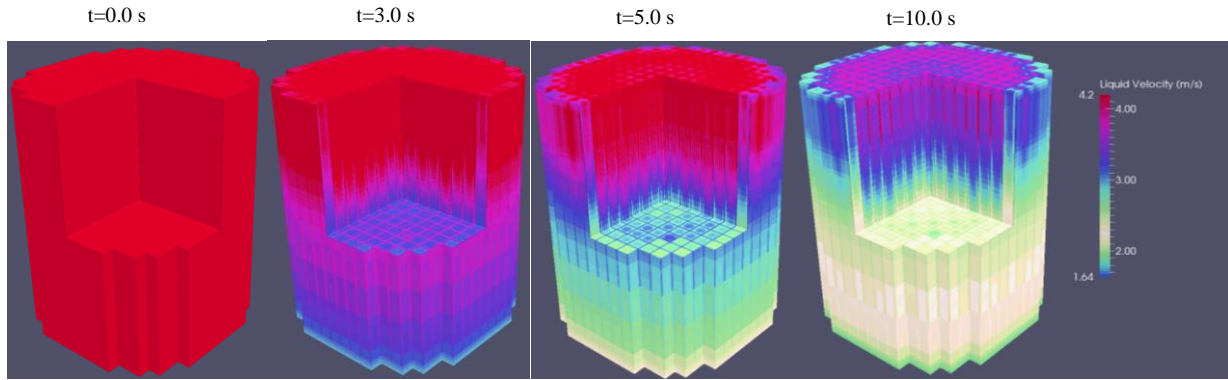


Figure 10. 3D Liquid Velocity at different transient times during LOF transient

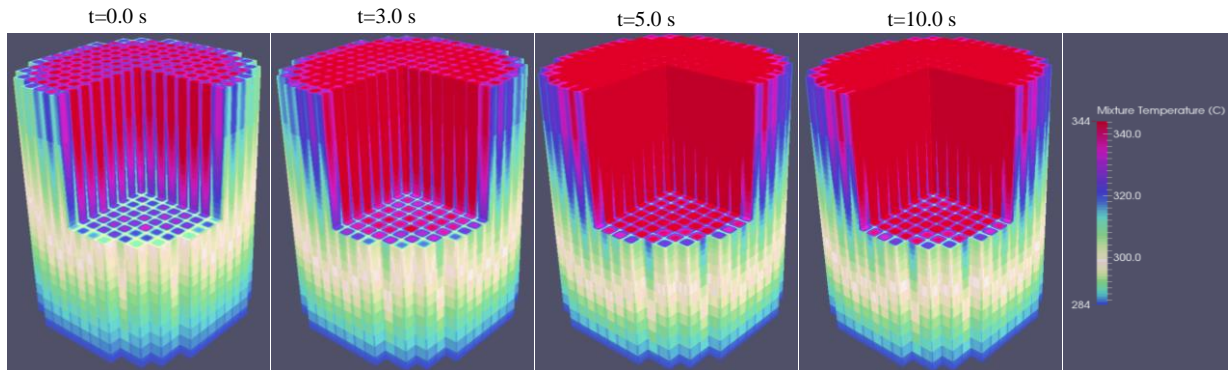


Figure 11. 3D Mixture Temperatures at different transient times during LOF transient

3.4 DNBR Prediction for Low Flow Steamline Break

The steam release resulting from a rupture of a main steam pipe on one of the steam generators will cause an increase in steam flow which decreases with time as the steam pressure decreases. The increased steam flow causes increased energy removal from the reactor coolant system (RCS) and results in a reduction of coolant temperature and pressure. The negative moderator temperature coefficient and the cooldown of the reactor system cause an increase in core reactivity. If the most reactive rod cluster control assembly (RCCA) is assumed stuck in its fully withdrawn position after reactor trip, there is an increased possibility that the core will become critical and return to power. A return to power following a steam line rupture is a potential problem mainly because of the high power peaking factors which exist, assuming the most reactive RCCA to be stuck in its fully withdrawn position. The core is ultimately shut down by the boric acid injection delivered by the safety injection system.

In this analysis, the rupture of a steam line was assumed in one of the three loops of the plant, which resulted in a highly asymmetric inlet coolant temperature and power distribution in the core. Because the most reactive RCCA was assumed in its stuck position coincident with the same region affected by the loop with steamline break, the power peaking factors were very high in that part of the core. Furthermore, it was assumed that the reactor was cooled by natural circulation after the reactor coolant pumps were shut down due to a loss of offsite power. The purpose of this analysis is to demonstrate that CTF is capable of simulating this challenging problem with its highly asymmetric power distribution and low pressure/low flow condition.

A previous steam line break analysis performed by Westinghouse provided a state-point at which the DNBR was found to be at its minimum value during the transient. This corresponded to a time when the RCS pressure was reduced to 580 psia, the core inlet flow rate was at 12% of the nominal flow rate, and the power was about 10% of the normal operating power.

Figure 12 shows the core and assembly radial power distributions input to the CTF calculation. As seen from the figure, the core power distribution was highly asymmetric; the high power assemblies were clustered in the broken loop section of the core. The hot assembly factor was about 7.2 and the hot channel factor was about 1.27. A top-peaked axial power profile, as seen in Figure 13, was assumed for every assembly in the analysis. Increased energy removal from the RCS due to increased steam flow in the broken loop was approximated using the inlet temperature distribution, as shown in Figure 14.

In the MSLB analysis, the effect of increased flow in the hot channel due to the phenomenon of “thermal siphoning,” or the “chimney effect” was accounted for by the open-channels modeled with CTF. Under the low flow natural circulation condition with a skewed radial power distribution, there was significant cross-flow from surrounding core region into the hot channel. The axial flow significantly increased from the channel inlet to the upper regions of the hot assembly. Figure 15 shows the liquid and vapor mass flow rates as a function of axial height. The axial flow rate increased towards the top of the hot channel where the boiling occurred. This chimney effect is demonstrated further in Figure 16 with the 3D mass flux distribution, which shows that there was even a small reverse flow at the top of the hot region.

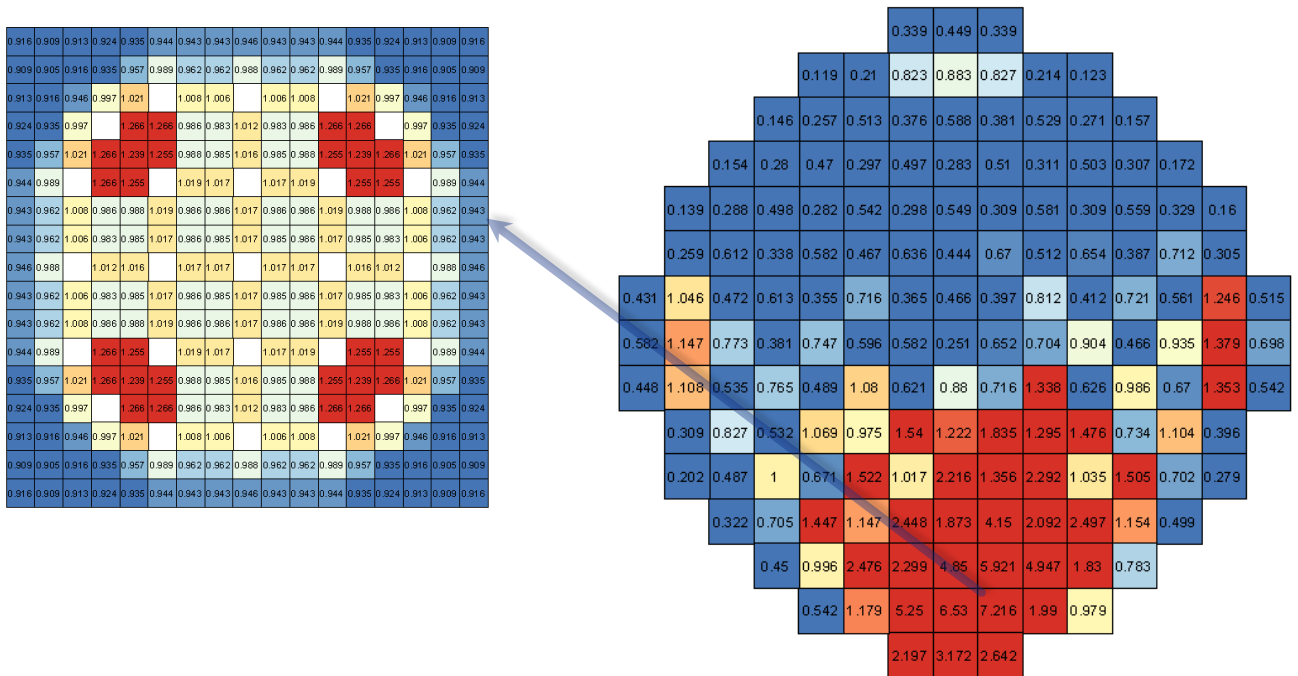


Figure 12. Assembly and Core Radial Power Distribution used for the MSLB Analysis

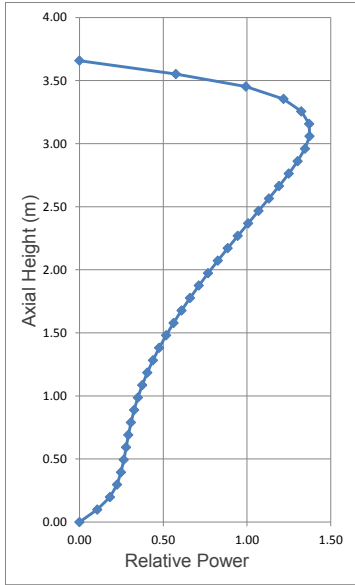


Figure 13. Axial Power Profile for MSLB Analysis

REGION	Tin(F)
1	404.85
2	397.32
3	387.33
4	374.98
5	370.05
6	364.83

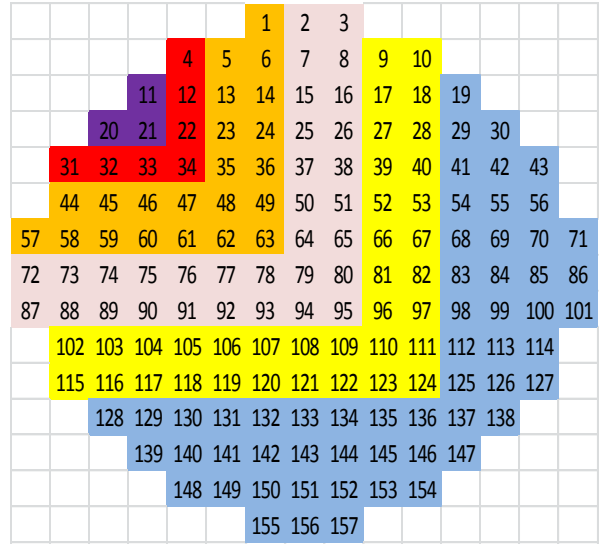


Figure 14. Inlet Temperature Distribution used in the MSLB Analysis

Figure 17 shows the hot channel and hot rod temperatures. Following the axial power shape, the liquid temperature reached saturation at around 90 inches (2.29m) from the bottom of the channel. In this low flow case, most power was generated in a small area of the core. The reduction in flow caused a rapid increase in enthalpy in the high powered assembly. Clad inner and outer surface temperatures also increased rapidly with varying slopes, depending on the heat transfer and flow regimes. Figure 18 further shows the 3D distribution of the mixture temperatures, demonstrating the enthalpy rise in the high powered regions.

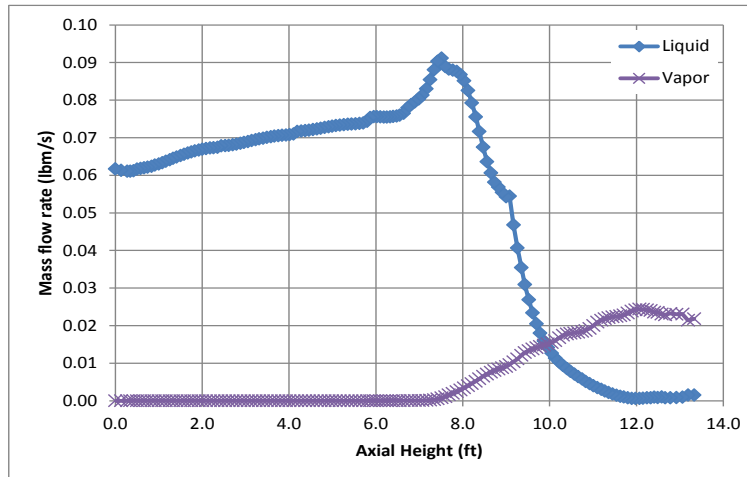


Figure 15. Hot Channel Liquid and Vapor Mass Flow Rates at MDNBR during the MSLB Transient

This steady-state problem was simulated on 157 compute nodes (1 fuel assembly/node), accessing the memory of 2 cores/node to accommodate the large problem size. A slow convergence rate was observed for this problem, requiring ~10,000 time steps. The total wall-clock time to achieve convergence was 4 hours 55 minutes.

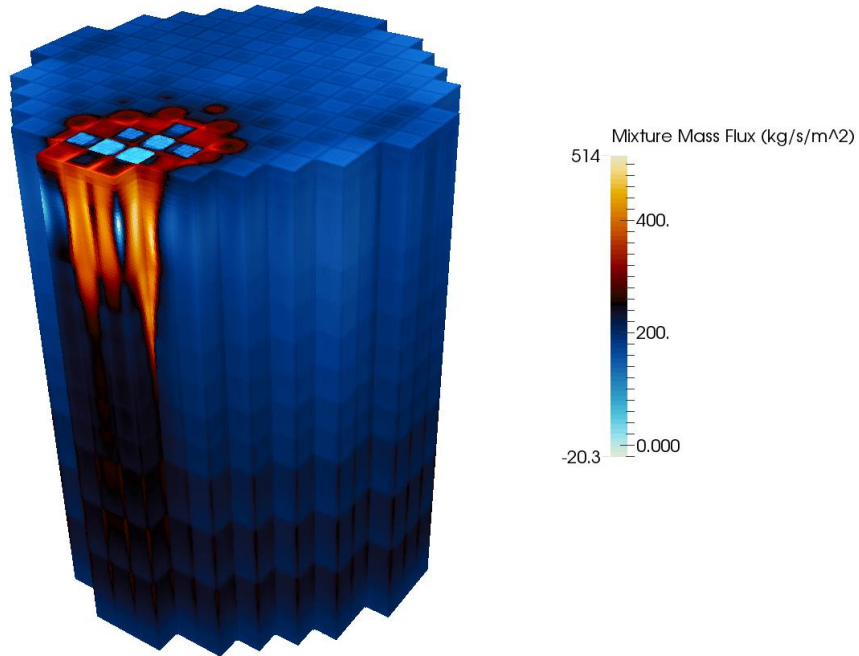


Figure 16. Mixture Mass Flux at MDNBR during the MSLB Transient

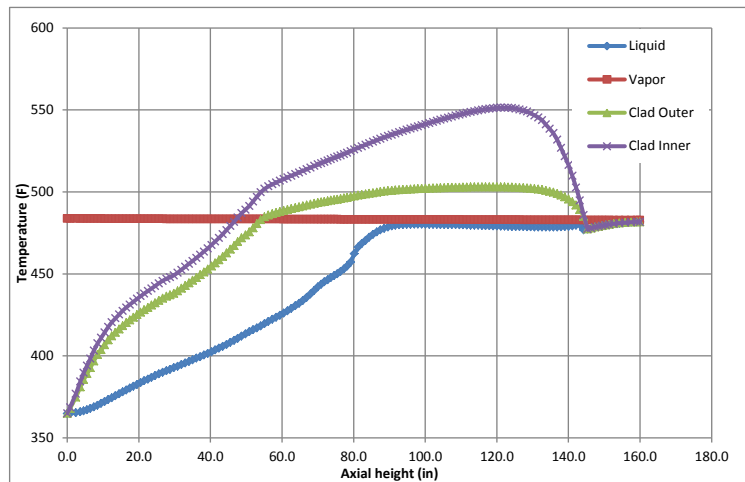


Figure 17. Hot Channel Temperatures Calculated in the MSLB Analysis

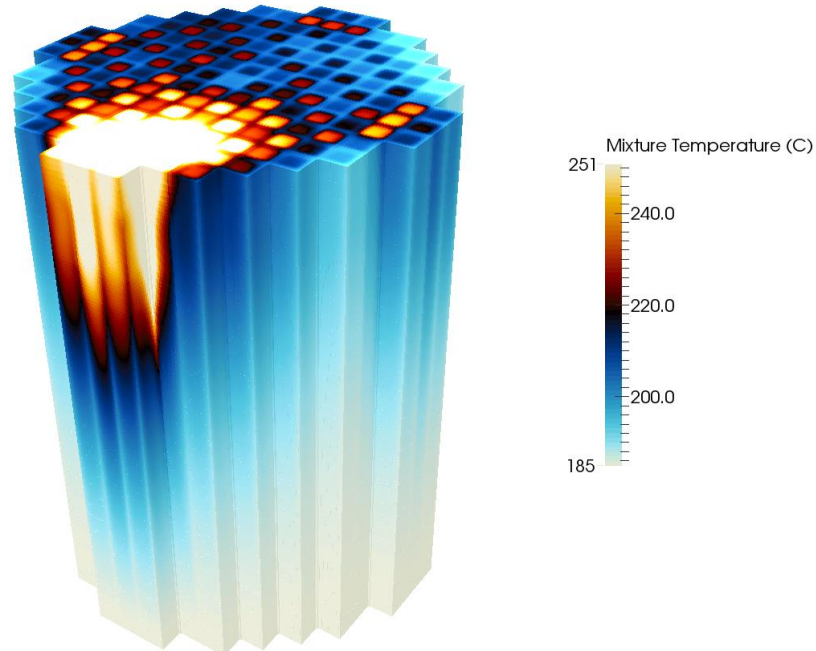


Figure 18. 3D Mixture Temperatures Calculated in the MSLB Analysis

3.5 DNBR Prediction for RIA at Power

An RCCA bank ejection at power event results in an increase in the core nuclear power that can result in fuel rods experiencing DNB. The 4-loop plant model described in Section 3.1 was used to simulate the RIA transient with the initial and boundary conditions given in Table II. During the 10 second transient, the RCS pressure, inlet temperatures, and inlet flow remained at initial values. In the first 5 seconds, the system was allowed to converge to a steady-state before the power transient forcing function was applied.

Figure 19 shows the power forcing function. The same core radial and assembly pin power distributions are applied here as in the loss-of-flow transient case. Although not accurate and realistic, the power distribution was not allowed to change during the transient for simplicity. The forcing function was applied as a global scaling factor to the initial power distribution.

With the RCCA ejection at full power, the core power rapidly increased. The power reached the peak at about 120% of the nominal power, and eventually, reactor was tripped. The minimum DNBR, also plotted in the same figure, showed a slight decrease from its initial value corresponding to the power increase. Because of its rapid nature and limited power increase, not much enthalpy was released from the fuel to the clad and coolant. As shown in Figure 20, a mild increase was observed in the channel and clad temperatures. Figure 21 shows the change in liquid enthalpy at the initial time step, at the time of minimum DNBR; and at the end of the transient. As shown in the 3D plots, there was little observable change in the enthalpy values between the initial time and the time of MDNBR.

This transient was simulated on 193 compute nodes (1 fuel assembly/node), accessing the memory of 2 cores/node to accommodate the large problem size. The total wall-clock time for this 10 second transient was ~ 7hours.

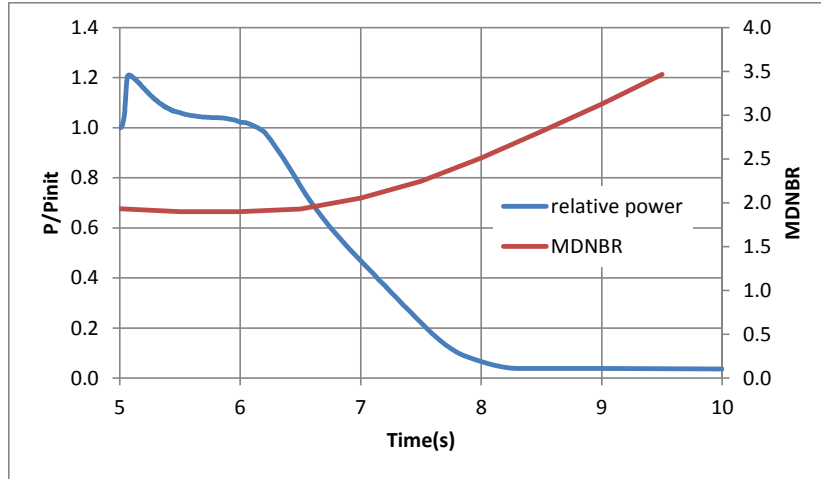


Figure 19. Transient Power Forcing Function and the Calculated MDNBR for the RIA Transient

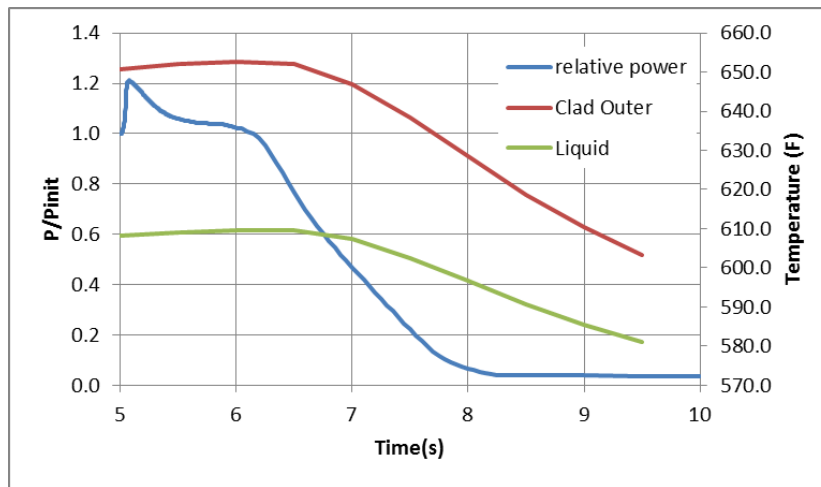


Figure 20. Clad and Liquid Temperatures in the Hot Channel Calculated for the RIA Transient

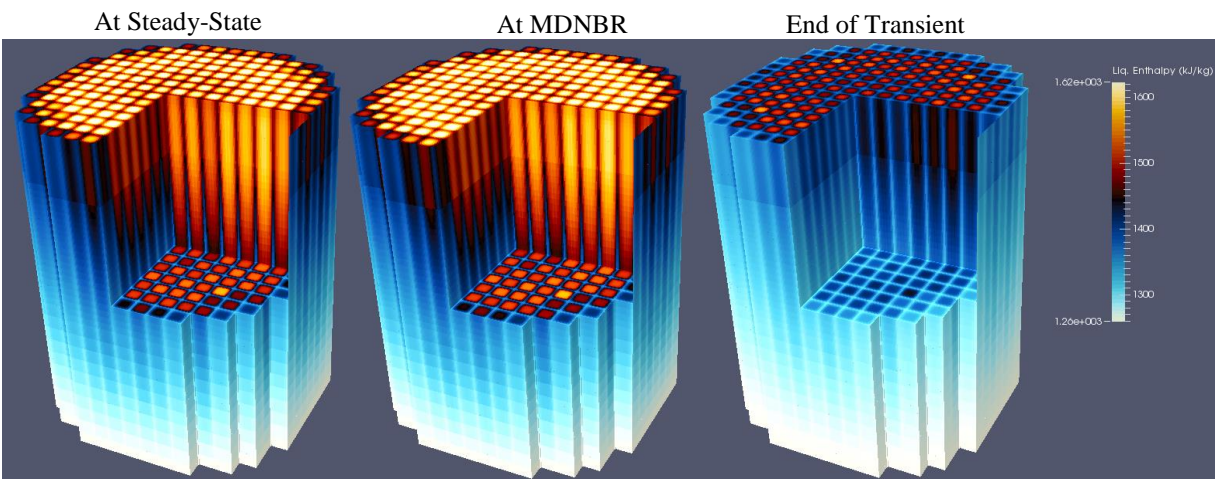


Figure 21. Core Liquid Enthalpies at Different Times during the RIA Transient

4 CONCLUSIONS

The CASL VERA-CS subchannel code CTF has been parallelized and a PWR preprocessor has been developed in order to support full reactor core modeling at coolant-channel resolution. This has been done to support PWR challenge problem modeling applications such as DNB. The code has been applied to predict DNB occurrences and core thermal responses during postulated PWR DNB accidents such as complete loss of forced coolant flow, main steamline break, and RCCA ejection at power. Full core 3D models of a 3-loop and a 4-loop PWR have been developed, modeled at coolant-channel resolution, leading to problem sizes of 6.9 and 8.5 million mesh cells, respectively. This study has demonstrated that CTF is capable of solving large, high-resolution models that relate to the specific CASL DNB challenge problem utilizing the newly developed PWR preprocessor and parallelization feature. These findings are important for future planned CTF activities, which include its use for coupled multi-physics analyses in the VERA-CS system.

This paper contains results of research supported by the Consortium for Advanced Simulation of Light Water Reactors (www.casl.gov), an Energy Innovation Hub (<http://www.energy.gov/hubs>) for Modeling and Simulation of Nuclear Reactors under U.S. Department of Energy Contract No. DE-AC05-00OR22725.

This research used resources of the Oak Ridge Leadership Computing Facility at the Oak Ridge National Laboratory, which is supported by the Office of Science of the U.S. Department of Energy under Contract No. DE-AC05-00OR22725.

5 REFERENCES

1. Avramova, M. *COBRA-TF Input Manual*. The Pennsylvania State University. 2014.
2. Salko, R. and Avramova, M. *CTF Theory Manual*. The Pennsylvania State University. 2014.
3. Montgomery, R., *VERA Tools and Workflows*, CASL Technical Report: CASL-U-2014-0054-001, March 2014.
4. Thurgood, M. et al. COBRA-TF Development. In *8th Water Reactor Safety Information Meeting*, Gaithersburg, Md. Oct. 1980.
5. Thurgood, M. et al. *COBRA/TRAC—A Thermal-Hydraulics Code for Transient Analysis of Nuclear Reactor Vessels and Primary Coolant Systems*. Technical Report NUREG/CR-3046, Pacific Northwest National Laboratory. 1983.
6. Paik, C. et al. *Analysis of FLECHT-SEASET 163-Rod Blocked Bundle Data using COBRA-TF*. Technical Report NUREG/CR-3046, United States Nuclear Regulatory Commission. 1985.
7. Pawlowski, R., Clarno, K., and Montgomery, R. *Demonstrate Integrated VERA-CS for the PCI Challenge Problem*. CASL Milestone Report CASL-I-2014-0153-000.
8. Bartlett, Ross, *TriBITS Developer's Guide and Reference*, CASL Technical Report, CASL-U-2014-0075-000-b, March 2014.
9. Salko, R. et al. *CTF Validation*. Oak Ridge National Laboratory. CASL-U-2014-0169-000. October 24, 2014.

10. Salko, R. et al. *Improvements, Enhancements, and Optimizations of COBRA-TF*. International Conference on Mathematics and Computational Methods Applied to Nuclear Science & Engineering (M&C 2013). Sun Valley, Idaho, USA. May 5-9, 2013.
11. Salko, R., et al. *Initial COBRA-TF Parallelization*. Consortium for Advanced Simulation of LWRs. CASL-I-2013-0180-000. August 21, 2013.
12. Balay, S. et al, *PETSc Users Manual*, ANL-95/11, January 2015.
13. Kucukboyaci, V., Cao, Liping, Y. Sung, *COBRA-TF Simulation of Fuel Thermal Response during Reactivity Initiated Accidents using the NSRR Pulse Irradiation Experiments*. ASME 2014 International Mechanical Engineering Congress & Exposition, Nov. 14-20, 2014, Montreal, Canada.
14. Salko, R. and Avramova, M. *CTF Pre-processor User's Manual*. The Pennsylvania State University. 2014.